Cationic Platinum(II) Complexes Bearing Aryl-BIAN Ligands: Synthesis, Structural and Optoelectronic Characterization

Cameron O'Brien,[a] *Michael Yin Wong,*[a] *David B. Cordes,*[a] *Alexandra M. Z. Slawin,*[a] *and Eli Zysman-Colman*[a]*

[a] EaStCHEM School of Chemistry, University of St Andrews, St Andrews, Fife, UK, KY16 9ST, Fax: +44-1334 463808; Tel: +44-1334 463826; E-mail: eli.zysman-colman@st-andrews.ac.uk; URL: http://www.zysman-colman.com

ABSTRACT. Five cationic platinum(II) complexes bearing a 2-(3'-substituted-aryl)pyridine cyclometalating ligand (C^N) and a neutral Ar-BIAN ligand have been synthesized: [Pt(ppy)(PhBIAN)]PF_6, **1**, [Pt(3Fppy)(PhBIAN)]PF_6, **2**, [Pt(3MeOppy)(PhBIAN)]PF_6, **3**, [Pt(3MeOppy)(4-FPhBIAN)]PF_6, **4**, [Pt(ppy)(4-MeOPhBIAN)]PF_6, **5**. All complexes have been characterized by NMR spectroscopy and mass spectrometry. Complexes **2** and **3** have been characterized by X-Ray crystallography. Structure-property relationships were established from UV-Visible spectroscopy and cyclic voltammetry studies. Interestingly, we found that when both the C^N and the Aryl-BIAN ligands contained electron-donating MeO groups the absorption spectrum for the platinum complex extended out to 650 nm. The electrochemical studies of these

complexes established that they are electronically compatible dye-molecules for dye-sensitized solar cells.

Introduction. Ionic late transition metal complexes have received much interest due to their useful photophysical and electrochemical properties. They are now widely used in myriad applications ranging from bioimaging and sensing,[1] solid-state lighting in the form of light-emitting electrochemical cells,[2] electrochemiluminescence measurements,[3] dye molecules for dye-sensitized solar cells,[4] photosensitizers for solar fuels[5] and photoredox catalysts for organic transformations.[6] Though luminescent cationic ruthenium(II) and iridium(III) complexes have been widely studied, cationic platinum complexes,[7] particularly of the form $[Pt(C\hat{}N)(N\hat{}N)]^+$ have received much less attention (where C^N is a cyclometalating ligand such as 2-phenylpyridine and N^N is a diimine ligand such as 2,2'-bipyridine). Bernhard and co-workers recently showed that cationic Pt complexes absorb out to 450 nm and phosphoresce with low intensity mainly from a long-lived ligand-centered (^{3}LC) state over a very narrow energy range (480-500 nm) in DMF solution. These complexes were found to exhibit two reversible reduction waves associated with electron injection into the π^*- system of the bipyridine N^N ligand; oxidation of the Pt(II) ion was not observed.[8] Swager and co-workers recently reported that cationic platinum complexes with pendant hydrocarbon chains adopt liquid crystalline and mechanochromic behavior due to strong Pt···Pt interactions that guide self-assembly.[9] Self-assembled aggregation of cationic platinum complexes into micelles, films and polymers was used by Slugovc and co-workers to turn on red luminescence in these structures.[10] The weak emission of [Pt(ppy)(dppz-COOH)]OTf was found to red-shift and dramatically increase in intensity when intercalated within G-quadruplex DNA (dppz-COOH = 11-carboxydipyrido[3,2-*a*:2′,3′-*c*]phenazine; ppyH = 2-phenylpyridine).[11] The nature of the emission of related cationic

Pt complexes had been historically ascribed to a metal-to-ligand charge transfer (^{3}MLCT) to the cyclometalating ligand[12] or the diimine ligand, despite the structured profile of the emission spectra[13] These assignments clash with the more recent structre-property study by Bernhard (*vide supra*).

Our group has focused on the development of panchromic absorbers using non-ruthenium late-transition metal complexes as potential replacement dye molecules for DSSCs. We recently reported that iridium(III) complexes bearing electron-rich aryl groups on the bis(aryliminoacenaphthene) ligand, of the form $[Ir(C^N)_2(Ar\text{-}BIAN)]PF_6$, absorb out past 800 nm.[14] In this study, we turn our attention to cationic platinum(II) bearing Ar-BIAN ligands. To the best of our knowledge, cationic Pt(II) Ar-BIAN complexes have not been previously reported though there are a few reports on neutral Pt(II) Ar-BIAN complexes and their applications in catalysis,[15] activation of CO_2,[16] and C-H bond activation.[17] Notably, Weinstein and Castellano have also studied the photophysical properties of $[Pt(Mes\text{-}BIAN)L_2]$ complexes, with L an acetylide, a thiolate or a chloride, and found them to be near-infrared emitters in DCM solution at room temperature (Mes-BIAN = bis(mesitylimino)acenaphthene).[18]

Results and Discussion.

Synthesis.

Five cationic complexes were targeted in order to rationally probe the effects of substitution of both the C^N and Ar-BIAN ligands on the photophysical properties of the complexes. Complexes **1-3** were synthesized in order to modulate the electron density of the Ar-BIAN ligand through incorportation of electron-donating and electron-withdrawing groups at the 4-position of the arylimino fragments. Complexes **3-5** were used to assess the impact of electronic

tuning of the aryl moiety of the substituted phenylpyridine ligand. Substitution at the 3-position of the phenyl ring was chosen in order maximally impact the strength of the Pt-C bond, and by extention modulation of the optoelectronic properties of the complexes. The targeted complexes were obtained in two steps. The platinum dimers were synthesized from the corresponding 2-arylpyridines and K_2PtCl_4 in refluxing 2-ethoxyethanol:water mixed solvent system (Scheme **1**). The dimers were isolated as yellow solids after precipitation with water from the reaction mixture and were immediately used in the subsequent cleavage step. Cationic platinum(II) complexes **1-5** were obtained in poor yield from the cleavage of the corresponding dichloro-bridged platinum dimer with two equivalents of Ar-BIAN ligand. Complexes were isolated as their hexafluorophosphate salt following anion metathesis with aqueous NH_4PF_6. Each complex was fully characterized by ^{1}H NMR and ^{19}F NMR, ESI-HRMS and melting point analyses. To confirm the structure and bonding about the platinum center, X-ray diffraction studies were carried out on **2** and **3**,

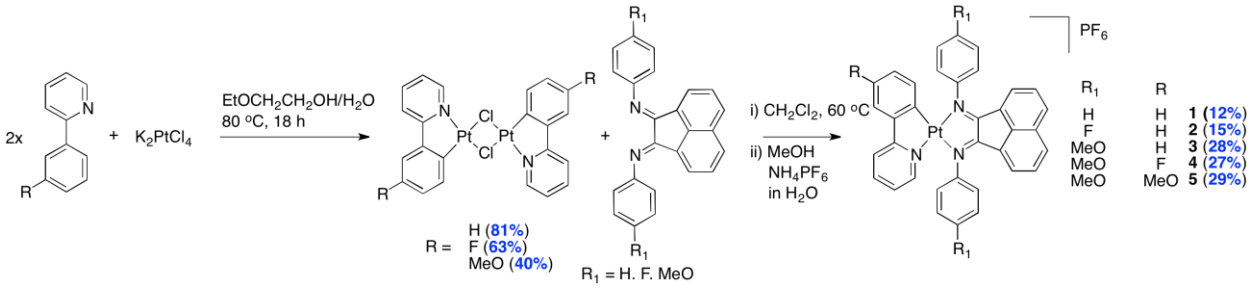

Scheme **1**. Synthesis of complexes in study.

X-Ray Structures.

Single crystals of both **2** and **3** were grown by vapor diffusion from a solution of CH_2Cl_2 and Et_2O (Figure **1**).[19] Complex **2** crystallizes as orange needles in the orthorhombic space group

*P*na2$_1$ while **3** crystallizes as red prisms in the triclinic space group $P\bar{1}$. The two complexes adopt a distorted square planar geometry and exhibit similar bond lengths and angles (Table **1**). Compound **2** includes a molecule of half-occupancy CH_2Cl_2 solvent.

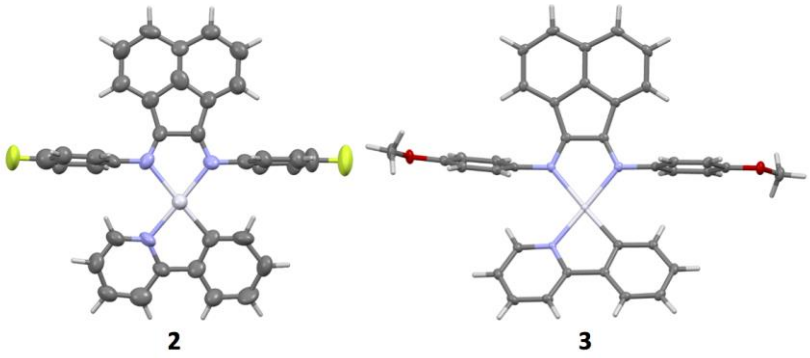

Figure **1**. Structure of the cationic complexes of **2** and **3**, thermal ellipsoids are drawn at the 50% probability level. The PF_6 counterion, solvent molecules and second disordered form of coordinating ppy N and C atoms in **3** eliminated for clarity

Table **1**. Selected bond lengths (Å). bond angles (°) and dihedral angles (°) for **2** and **3**.

complex	**2**	**3**
Pt-$N_{Ar\text{-}BIAN}$	2.07(1), 2.15(1)	2.109(2), 2.099(2)
Pt-N_{ppy}	2.03(1)	2.021(2)
Pt-C_{ppy}	1.99(1)	2.021(2)
Pt···Pt	7.218(2)	5.2853(7)
$N_{Ar\text{-}BIAN}$-Pt-$N_{Ar\text{-}BIAN}$	77.7(4)	78.38(8)
N_{ppy}-Pt-C_{ppy}	80.9(5)	79.93(9)
$N_{Ar\text{-}BIAN}$-Pt-N_{ppy}	100.6(5)	100.06(9)
$N_{Ar\text{-}BIAN}$-Pt-C_{ppy}	100.5(5)	101.09(9)

C_{Ar}-$N_{Ar\text{-}BIAN}$-C_{Ph}-C_{Ph}	96(2), 85(2)	86.7(3), 75.4(3)

Despite the different coordination geometries, the bite angles are very similar to the analogous octahedral Ir(III) complexes [Ir(ppy)$_2$(Ar-BIAN)], where Ar = 4-MeOPh and 4-MeO$_2$CPh (80 – 81^o for C_{ppy}-Pt-N_{ppy} versus 80^o for C_{ppy}-Ir-N_{ppy} and 78^o for $N_{Ar\text{-}BIAN}$-Pt-$N_{Ar\text{-}BIAN}$ versus 76^o for $N_{Ar\text{-}BIAN}$-Ir-$N_{Ar\text{-}BIAN}$).[14] Bond lengths in **2** and **3** are by contrast slightly shorter (Pt-C_{ppy}, Pt-N_{ppy} and Pt-$N_{Ar\text{-}BIAN}$ averaging 2.00, 2.03 and 2.11 Å, respectively, versus Ir–C_{ppy}, Ir–N_{ppy} and Ir–$N_{Ar\text{-}BIAN}$ averaging 2.01, 2.05 and 2.17 Å) due to the *trans* influence of the Ar-BIAN and ppy nitrogen atoms in **2** and **3**. The bond lengths from the Pt atom to the cyclometalating 2-phenylpyridine are comparable to those found in previously reported C^N chelate Pt(II) compounds of the form [Pt(C^N)(acac)], where acac is acetylacetonate (Pt-N 1.986 – 2.02 Å and Pt-C 1.939– 2.08 Å).[20] The Pt-$N_{Ar\text{-}BIAN}$ bond lengths are intermediate compared to those found in neutral [Pt(Mes-BIAN)(CCAr)$_2$] complexes studied by Weinstein[18b] and co-workers (Pt-$N_{Mes\text{-}BIAN}$ 2.019 – 2.098 Å), and [Pt(Ar-BIAN)(OH)$_2$] studied by Parvez[16] and co-workers (Pt-N 2.035 – 2.213 Å).

Both the acenaphthylene component of the Ar-BIAN and the 2-phenylpyridine ligands adopt near-planar arrangements, the 2-phenylpyridines being distorted further from planarity. However, these two ligand components are not arranged in a coplanar manner, the angle between the planes formed being 14.7° and 33.1° for **2** and **3**, respectively. This leads to a more bowed appearance for **3** in comparison to **2**. In a similar arrangement to the conformation observed in Ar-BIAN-containing iridium(III) complexes, the aryl groups of the Ar-BIAN ligand are oriented

nearly orthogonal to the plane of the acenaphthylene component (for **2** 81.6° and 85.2°, for **3** 82.5° and 98.5°), thereby promoting intramolecular CH-π interactions with both the α-protons of the ppy ligand and the adjacent protons of the acenaphthylene ring.

The packing of the two complexes falls into two different modes, leading to significant differences in the internuclear Pt···Pt distances (Figure **2** and Table **1**). In complex **2**, chains of complexes running along the *c*-axis are formed by an offset π-stacking arrangement between the acenaphthene fragment of one molecule with the ppy of a second. These chains of complexes further pack in a pseudo-herringbone configuration with the adjacent chain, interacting with it *via* CH···π interactions between ppy ligands (Figure **2**). These pairs of chains interact with each-other by means of weak CH···F hydrogen bonds, involving fluorine atoms from both the Ar-BIAN ligand and PF_6^- anion. This creates channels running along the *c*-axis, which are occupied by the CH_2Cl_2 solvent molecules. In contrast, complex **3** appears to be unable to form similar π-stacks, possibly due to the less planar arrangement of its two ligands. Instead, it forms dimers of complexes, linked together by a pair of CH···π interactions, and PF_6^- anion bridging CH···F interactions (Figure **2**). These dimers then pack together, interacting by means of a complex network of further CH··π, and CH···O and CH···F hydrogen bonds. The offset of the π-stacking in **2** means that the shortest internuclear Pt···Pt distance in the crystal structure is between platinum atoms in adjacent chains, at 7.218(2) Å. In contrast, due to much greater overlap between dimers of complexes in the crystal structure of **3**, the shortest Pt···Pt distance in this complex is between platinum atoms in a dimer arrangement, at 5.2853(7) Å.

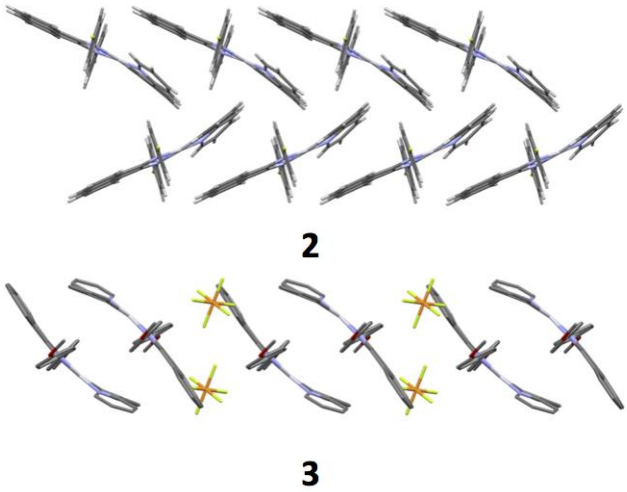

Figure **2**. Views of the backing of complexes **2** and **3**, hydrogen atoms were omitted for clarity. (Two adjacent chains of π-stacking complexes of **2**, interacting via CH···π contacts, running along the *c*-axis. The PF_6^- anion and CH_2Cl_2 solvent molecules were omitted. Dimers of complex **3**, interacting via CH···π contacts. The PF_6^- anions involved in linking adjacent dimers are shown.

Solution State Structures.

The aromatic regions of the ^{1}H NMR spectra of **1-3** in CD_3CN are shown in Figure **3a**. Unlike in the iridium complexes, where the α protons on the Ar-BIAN are shifted significantly upfield to around 6.1 ppm and present as a doublet,[14b] these protons now are found significantly downfield at around 7.1 ppm and are now chemically non-equivalent due to the lack of symmetry in the complex and exist for most complexes as an apparent triplet. In **4**, the α and α' protons show as broad multiplets at 7.08 and 6.90 ppm. Indeed, α and α' protons have been found to be significantly deshielded in other [Pt(Ar-BIAN)LL'] complexes.[15a,16-17,21] The γ protons are shifted slightly further downfield relative to the ^{1}H NMR spectra of the corresponding iridium complexes and free ligands.[14b,22] However, substitution of electron rich

aryls on the Ar-BIAN ligand leads to downfield shift of both the α and γ protons, while with the iridium complexes, the α proton was found to shift upfield with increasing electron density on the aryl moieties of the Ar-BIAN ligand.[14b]

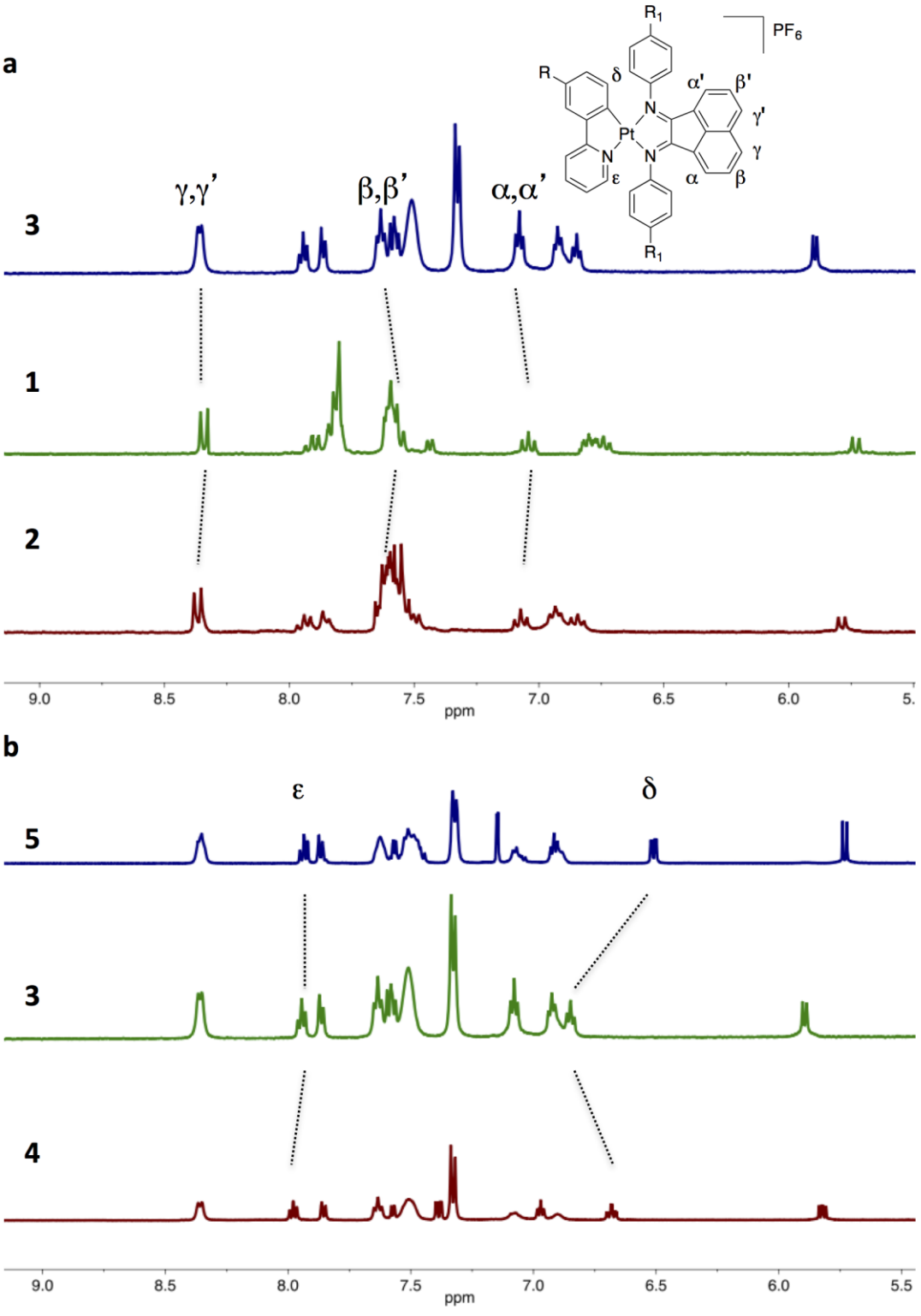

Figure **3**. Aromatic region of in CD_3CN at 298 K for a) **1-3** and b) **3-5**.

The aromatic region of the ^{1}H NMR spectra of **3-5** in CD_3CN are shown in Figure **3b** and illustrate the effect of substitution on the aryl moiety of the C^N ligand. The similarities in the ^{1}H NMR spectra point to a similar substitution pattern on the C^N ligand. We have inferred that the substitution is *para* to the Pt-C bond due to similar NMR patterns in octahedral iridium complexes bearing similar C^N ligands and do the the steric crowding that would occur in the case where the substituent on the phenyl ring was *ortho* to the Pt-C bond; Jones,[23] however, has isolated regioisomeric mixtures in both iridium and rhodium complexes of the form [M(C^N)Cp*Cl] where C^N is a 3-substituted phenylpyridine and M = Ir or Rh and concluded that C-H activation in these cases was reversible though slow. There is a significant upshift of the δ proton adjacent to the cyclometalating carbon in **5** and a somewhat smaller upfield shift of this proton in **3** resulting from the mesomeric electron donation of the MeO and F substituents, respectively. Conversely, the environment of the ε proton adjacent to the nitrogen atom of the pyridine ring is only slightly perturbed.

Cyclic voltammetry. The electrochemistry of **1-5** was assessed through cyclic voltammetry (CV) studies in deaerated MeCN solution containing *n*-NBu_4PF_6 as the supporting electrolyte and using Fc/Fc^+ as an internal standard at 298 K. All potentials are referenced to NHE (Fc/Fc^+ = 0.63 V in MeCN).[24] The electrochemistry data, obtained at a scan rate of 50 mV s^{-1}, are shown in Table **2**. The CV behavior was largely reproducible at faster scan rates of 100, 200 and 1000 mV s^{-1}. The CV traces for **1-5** are shown in Figure **4**.

Table **2**. Relevant electrochemical data for complexes **1-5**.[a]

complex	E^2_{ox}[b]	E^1_{ox}[b]	$E^1_{1/2,red}$	ΔE_p	$E^2_{1/2,red}$	ΔE_p	ΔE[c]	$E_{0,0}$	$E(S^+/S^*)$[d]

	V	V	V	mV	V	mV	V	eV	eV
1	1.55	0.93	-0.19	80	-0.94	90	1.08	2.20	-1.27
2	1.72	1.07	-0.16	80	-0.90	90	1.19	2.14	-1.07
3	1.52	0.87	-0.22	60	-0.96	90	1.06	2.13	-1.26
4	1.58	0.96	-0.21	80	-0.98	120	1.13	2.16	-1.20
5	1.51	0.85	-0.24	70	-0.80	90	1.05	1.86	-1.01

[a] Conditions: Recorded in N_2-saturated MeCN with 0.1 M (nBu$_4$N)PF$_6$ and referenced internally to Fc/Fc$^+$ at a scan rate of 50 mV/s. Potentials are versus NHE (Fc/Fc$^+$ vs NHE = 0.63 V).[24] A nonaqueous Ag/Ag$^+$ was used as the pseudoreference electrode, a glassy carbon electrode was used as the working electrode, and a Pt electrode was used as the counterelectrode; [b] Irreversible oxidation waves, E_{pa} reported. [c] $\Delta E_{redox} = \Delta E = E^1_{ox} - E^1_{pa,red}$; [d] Calculated from $E(S^+/S^*) = E^1_{ox} - E_{0,0}$, where $E_{0,0}$ is estimated from the onset of the absorption spectrum at ca. 10% intensity.

The first oxidation waves for **1-5** lie between 0.85 V and 1.05 V and are irreversible. In the present study, this oxidation wave is at much lower positive potential than observed in previous work on iridium(III)[14] (E_{ox}: 1.22 – 1.60 V) and platinum(II)[18a,18b] Ar-BIAN complexes (E_{ox}: 0.95 – 1.35 V) and platinum(II) complexes containing a C^N ligand (E_{ox}: 0.96 – 1.35 V).[25] These oxidation potentials are however in line with other neutral platinum(II) complexes that have been investigated as dyes for DSSCs.[26] Based on these previous studies, the HOMO is assigned to be located on the Pt and the C^N ligand. The irreversible nature of this oxidation wave is due to the instability of the Pt(II)/Pt(III) couple, which is oxidised and reduced by the solvent.[27] However, there is a strong effect on the oxidation potential through substitution on the Ar-BIAN ligand,

suggesting that this ligand too is involved in the HOMO. For instance, the addition of an electron-withdrawing F atom in **2** promotes a 140 mV anodic shift compared to **1** while the presence of an electron-donating MeO group in **3** results in a 60 mV cathodic shift. Substitution at the 3-position of C^N ligand leads to the same trend but to a less pronounced degree (110 mV anodic shift for electron-withdrawing F substitution and 20 mV cathodic shift for electron-donating MeO substitution), suggesting that contribution from this fragment is less important though still implicated in the oxidation process.

The second irreversible oxidation wave lies between 1.51 V and 1.72 V. Due to the similar structure-property trends observed, this oxidation is also proposed to implicate the platinum metal center, and both the Ar-BIAN and the C^N ligands.

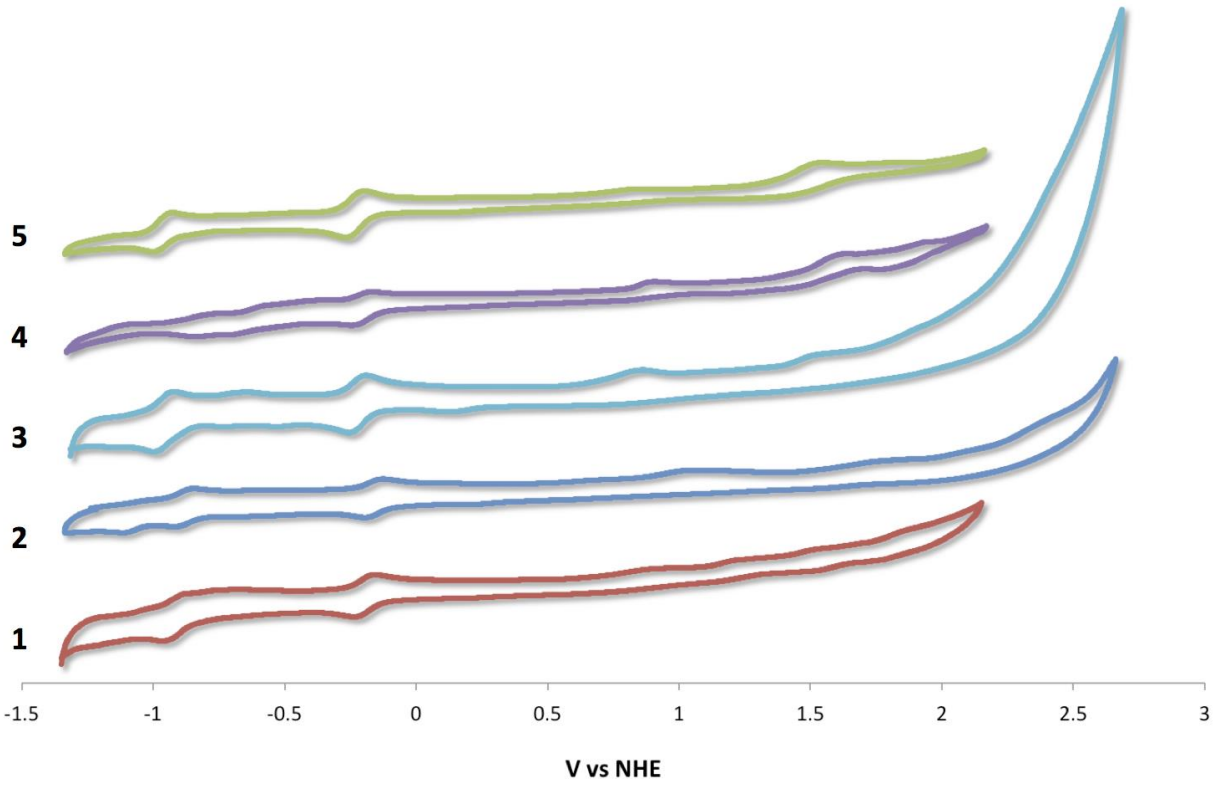

Figure **4**. Cyclic voltammograms for **1-5** in MeCN with 0.1 M (nBu$_4$N)PF$_6$ recorded at room temperature at 50 mV s^{-1}.

The first reduction wave in **1-5** was found to be reversible and to lie between -0.16 V and -0.24 V . These reduction potentials are significantly anodically shifted compared to those previously reported by Weinstein[18a,18b] for Pt Ar-BIAN complexes (E_{red}: -0.92 – -1.03 V) but are in line with those for cationic Ir Ar-BIAN complexes[14b] (E_{red}: -0.29 – -0.57 V) and result from a reduction of the Ar-BIAN ligand. The substitution of the C^N showed limited effect on the reduction potential with a 30 mV maximum variation between **3-5**.

The structure-property trends observed for the first reduction wave are mostly emulated with the second reduction **1-4**. For **5** the second reduction wave is anodically shifted to -0.80 V, suggesting a change in the nature of this reduction process, and implicating a much larger contribution from the electron-rich C^N ligand. The electrochemical gap, ΔE_{redox}, ranges from 1.05 V for **5** to 1.19 V for **2**.

The optical gap, $E_{0,0}$, approximates the HOMO-LUMO gap, which is between 1.86 and 2.20 eV for these complexes. The corresponding excited state oxidation potentials, $E(S^+/S^*)$, were calculated to lie between -1.01 to -1.26 eV. Notably, these values are sufficiently energetic to inject into the TiO_2 conduction band (<-0.5 V), making these complexes energetically compatible dyes for DSSCs.

Electronic spectroscopy. The UV-visible absorption spectra for **1-5** were recorded in aerated MeCN at 298 K. The spectra are shown in Figure **5** and the calculated molar absorptivities, ε, for

the absorption bands are summarized in Table **3**. As has been seen with previous Pd, Pt, Cu, Zn and Ir Ar-BIAN complexes,[14a,18b,28] the absorption spectra are red-shifted compared to the free Ar-BIAN ligands. The high energy high intensity bands (> 300 nm) are $\pi \rightarrow \pi^*$ transitions on both the Ar-BIAN and C^N ligands.[18b,18c] The two distinctive absorption bands around 330 and 460 nm result from mixed metal-to-ligand charge-transfer and ligand-to-ligand charge-transfer (^{1}MLCT/^{1}LLCT) transitions.[14,18a,18b,29]

Table **3**. UV-visible Absorption data.[a]

	λ_{abs} /nm (ε /10^4 M^{-1} cm^{-1})
1	270 (1.96), 313 (1.28), 323 (1.29), 360 (0.93), 420 (0.36), 450 (0.39)
2	260 (2.18), 311 (1.45), 325 (1.47), 358 (1.26), 420 (0.53), 462 (0.65)
3	273 (1.83), 312 (1.19), 325 (1.22), 363 (0.95), 425 (0.60), 455 (0.66)
4	270 (2.03), 311 (1.36), 325 (1.49), 345 (1.47), 360 (1.25), 425 (0.68), 450 (0.79)
5	280 (2.54), 314 (2.24), 360 (1.42), 460 (0.88), 600 (0.23)

[a] Absorption spectra recorded in air-equilibrated MeCN at 298 K.

The absorption profiles for **1-5** between 300 and 400 nm exhibit three separate bands. These three bands are not affected by substitution on the Ar-BIAN ligand. On the other hand, the two closely spaced high energy bands become less-well resolved and are slightly blue-shifted in **5** while being red-shifted in **4** compared to **3**, thus implicating a transition with significant C^N character. The lower energy band in **5** is somewhat red-shifted broader, tailing out to 370 nm.

In the region between 400 and 500 nm, there is a modest blue-shift in the absorption profile of **3** and a larger red-shift in the profile of **2** compared to **1**, pointing to a modulation of an occupied MO localized on the Ar-BIAN ligand for this transition. While the absorption profiles in this energy region for **3** and **4** are very similar, these bands are red-shifted in **5**, suggesting a change in the nature of these transitions to involve the C^N ligand. Notably, for **5** there is an additional weak absorption band centred at about 600 nm (ε = 2440 M^{-1} cm^{-1}). The presence of a similar band in the absorption spectrum of $[Ir(ppy)_2(4\text{-MeOPh-BIAN})]PF_6$ was attributed to increased through-space interaction between the aryl groups on the Ar-BIAN and the C^N ligand, resulting in increased intensity of LLCT transition.[14] The presence of the MeO group on the C^N ligand in **5** extends this chromophore and enhances the probability of this lowest energy transition.

The absorption profiles of **1-4** are similar to those previously reported by Weinstein and co-workers for neutral Pt Ar-BIAN complexes.[18a,18b] However, in the present study the absorption band centered around 450 nm is blue-shifted by about 65 nm. The low energy absorption band at 600 nm in **5** is not present in the literature examples.

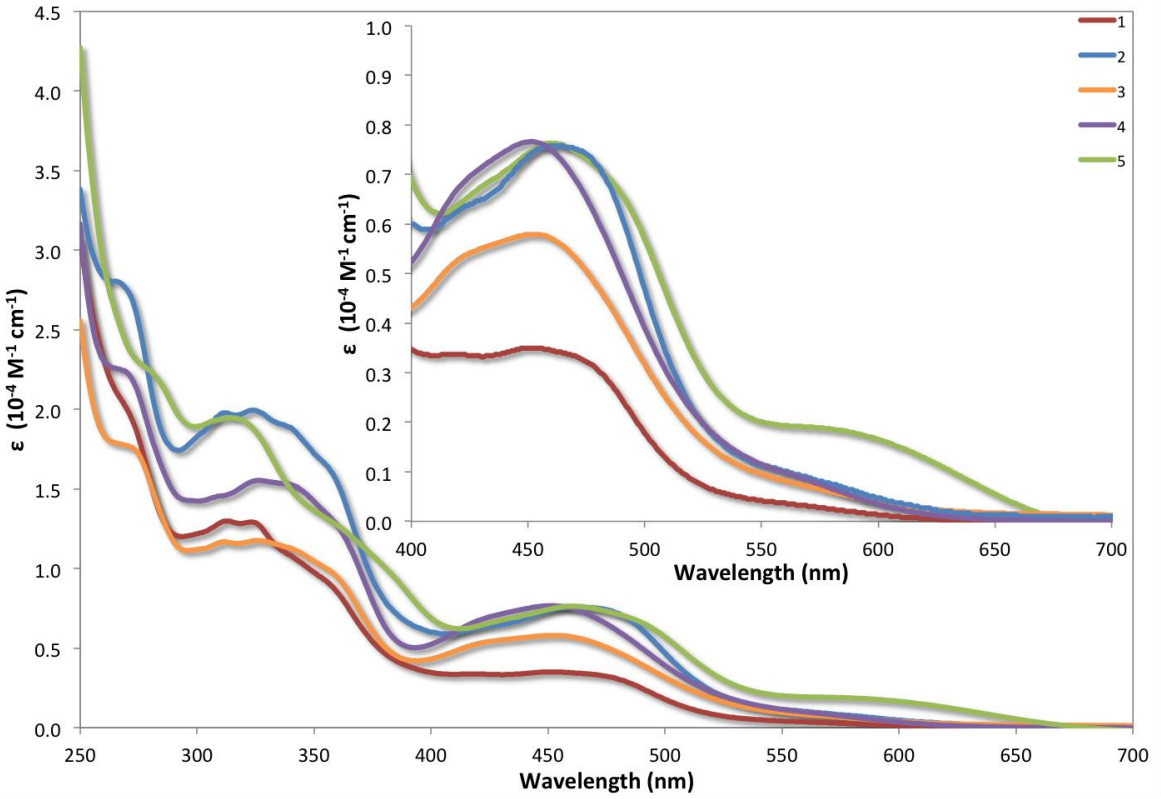

Figure **5**. UV-visible absorption spectra for **1-5** in MeCN at 298 K. Insert: Absorption spectra for low energy region.

No emission was detected out to 800 nm for **1-5** at both 298 and 77 K upon excitation at 365 nm under de-aerated conditions. It is possible that very low energy emission could exist[18c,30] and further efforts to check emission past 800 nm are presently underway. However, non-radiative deactivation through distortion of the square-planar structure towards tetrahedral has also been observed in platinum(II) complexes.[31]

Conclusions.

Herein we have reported a series of novel, absorptive cationic platinum(II) complexes bearing a substituted 2-phenylpyridine cyclometalating ligand and a Ar-BIAN diimine ligand. These

complexes were obtained in low yields (12 – 25%). X-ray structural analysis on two of these complexes, **2** and **3**, unambiguously confirmed their square planar geometry and structure.

The electronic and electrochemical properties of **1-5** were investigated. The absorption profiles showed absorption out to 650 nm, with molar extinction coefficients on the order of 10^4 M^{-1} cm^{-1}. The addition of electron-withdrawing and electron-donating groups on both the C^N and Ar-BIAN ligands was explored and structure-property relationships were established. A combination of electron-donating methoxy substitution on both ligands in **5** resulted in the largest observed red-shift of the absorption spectrum. The oxidation waves were found to be irreversible while the reduction waves were found to be reversible. The first oxidation wave, corresponding to the HOMO, lies between 0.85 and 1.07 V while the excited state oxidation potentials were found to be between -1.01 and -1.27 V. Though the optical gaps for these complexes are larger than would be preferable (1.86 – 2.20 V) for dyes for DSSCs, the orbital energies satisfy the requirements for their use in DSSCs. Efforts are presently ongoing to modify the Ar-BIAN ligand to incorporate an adsorbing unit, which would have the expected benefit of pushing the absorption further to the red.

Acknowledgements. EZ-C acknowledges the University of St Andrews for financial support.

Supporting Information. X-ray crystallographic data for **2** and **3** in CIF format. Tables of crystallographic refinement parameters and geometric features for **2** and **3**. ^{1}H NMR and ^{19}F NMR spectra for **1-5**. Individual cyclic voltammetry traces for **1-5**. This material is available free of charge via the Internet at http://pubs.acs.org.

Experimental Section

General Synthetic Procedures. Commercial chemicals were used as supplied. All reactions were performed using standard Schlenk techniques under an inert (N_2) atmosphere. Where freshly distilled anhydrous solvents were obtained they were from a Pure Solv^{TM} solvent purification system from Innovative Technologies. Flash column chromatography was performed using silica gel (Silia-P from Silicycle, 60 Å, 40-63μm). Analytical thin layer chromatography (TLC) was performed with silica plates with aluminium backings (250 μm with indicator F-254). Compounds were visualised under UV light. ^{1}H, ^{19}F and ^{13}C NMR spectra were recorded on either a Bruker Avance spectrometer at 300 MHz, 100 MHz and 75 MHz, respectively or a Bruker Avance III HD spectrometer at 500 MHz, 471 MHz and 126 MHz, respectively. The following abbreviations have been used for multiplicity assignments: "s" for singlet, "d" for doublet, "t" for triplet, "m" for multiplet, and "br" for broad. Spectra were referenced to the solvent peak. Melting points (Mp) were recorded using open-end capillaries on a Electrothermal melting point apparatus and are uncorrected. High-resolution mass spectra were recorded on a quadrupole time-of-flight (ESI-Q-TOF), model ABSciex 5600 Triple TOF in positive electrospray ionization mode and spectra were recorded using sodium formate solution as calibrant.

General Procedure for the formation of arylboronic acids. Adapted from a protocol by Reider and co-workers.[32] The aryl halide (5.37 mmol, 1 equiv.) was charged in dry toluene (9.5 mL) and THF (2.5 mL) and cooled to -78 ^{o}C. *n*BuLi (2.5 M in hexanes, 3.8 mL, 6.08 mmol, 1.15 equiv.) was then added dropwise over 10 minutes and the mixture allowed to stir for a further 20 minutes at -78 ^{o}C. Tri*iso*propyl borate (1.14 g, 6.07 mmol, 1.15 equiv.) was then added and the

reaction allowed to rise to -20 ^{o}C before HCl (1M, 7 mL) was added and the reaction allowed to reach room temperature. The reaction phases were separated and the organic phase dried and solvent removed under reduced pressure, resulting in white powder.

3-Fluorophenylboronic acid. White powder (0.70 g). **Yield:** 80 %. **Mp:** 187 – 188 ^{o}C. **Litt.:** 211 - 213 ^{o}C.[33]

3-Methoxyphenylboronic acid. White powder (0.75 g). **Yield:** 92 %. **Mp:** 152 – 154 ^{o}C. **Litt.:** 158 ^{o}C.[34]

General procedure for the synthesis of arylpyridines. Adapted from a protocol by Rabe and co-workers synthesis.[35] $Pd(PPh_3)_4$ (5 mol%) was added to a degassed solution of 2-bromopyridine (3.8 mmol, 1 equiv.) , K_2CO_3 (10.8 mmol, 3 equiv.), and boronic acid (4.94 mmol, 1.3 equiv.) in the dioxane (35 mL) and water (8 mL). The mixture was then degassed and heated to reflux for 18 h. Water was then added and the product extracted from DCM (20 mL). The crude oil was purified by chromatography (hexane/diethyl ether, 90/10%).

2-(3-methoxyphenyl)pyridine (3MeOppy):

Yellow oil (0.570 g). **Yield:** 81%. **R_f:** 0.4 (10% Hexane/Et_2O). **^{1}H NMR (300 MHz, $CDCl_3$) δ (ppm):** 8.70 (dt, *J* = 4.8, 0.9 Hz, 1H), 7.79 – 7.69 (m, 2H), 7.59 (dd, *J* = 2.6, 1.6 Hz, 1H), 7.58 – 7.52 (m, 1H), 7.38 (t, *J* = 7.9 Hz, 1H), 7.23 (ddd, *J* = 6.2, 4.8, 2.2 Hz, 1H), 6.97 (ddd, *J* = 8.2, 2.6, 1.0 Hz, 1H), 3.89 (s, 3H). Compound characterization matched those found in the literature.[36]

2-(3-fluorophenyl)pyridine (3Fppy):

Yellow oil (0.150 g). **Yield:** 63%. **R_f:** 0.4 (10% Hexane/Et_2O). **^{1}H NMR (500 MHz, $CDCl_3$) δ (ppm):** 8.62 (td, *J* = 4.7, 4.2, 2.2 Hz, 1H), 7.67 (dddd, *J* = 18.4, 10.8, 3.9, 2.1 Hz, 4H), 7.35 (ddd, *J* = 8.3, 4.0, 2.2 Hz, 1H), 7.18 (dtd, *J* = 6.7, 3.5, 1.8 Hz, 1H), 7.07 – 7.00 (m, 1H). **^{19}F NMR (471 MHz, $CDCl_3$) δ (ppm):** 113.02 (s). **^{13}C NMR (126 MHz, $CDCl_3$) δ (ppm):** 164.21 , 162.26 , 155.87 , 149.64 , 141.61 (d, *J* = 7.3 Hz), 136.89, 130.18 (d, *J* = 8.2 Hz), 122.64 , 122.35 (d, *J* = 2.8 Hz), 115.70 (d, *J* = 21.3 Hz), 113.76 (d, *J* = 22.8 Hz). Compound characterization matched those found in the literature.[36]

General procedure for the synthesis of [Pt(C^N)Cl]$_2$ dimers.

Adapted from a protocol Thompson and co-workers.[27a] K_2PtCl_4 (0.48 mmol, 1 equiv.) was heated with the substituted phenylpyridine, C^N, (1.2 mmol, 2.5 equiv.) in a mixture of 3:1 2-exthoxyethanol and water (20 mL) for 18 h at 80 ^oC. Water (40 mL) was added to the reaction mixture and the resulting yellow precipitate was isolated by filteration.

[Pt(ppy)(μ-Cl)]$_2$:

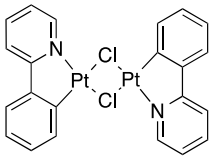

Yellow crystals (0.200 g). **Yield:** 81%. **Mp:** 212 – 214 ^oC.

[Pt(3Fppy)(μ-Cl)]$_2$:

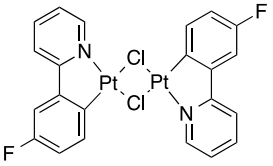

Yellow crystals (0.150 g). **Yield:** 63%. **Mp:** 298 – 300 ^oC.

[Pt(3MeOppy)(μ-Cl)]$_2$:

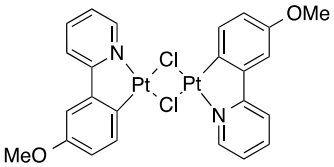

Yellow crystals (0.020 g). **Yield:** 40%. **Mp:** 200 – 201 ^{o}C

*General procedure for the synthesis of bis(arylimino)acenaphthenes (Ar-BIANs). A*dapted from a protocol by Hasan and Zysman-Colman.[22a] Acenaphthene (2.74 mmol, 1 equiv.) and anhydrous $ZnCl_2$ (7.34 mmol, 2.7 equiv.) were charged under nitrogen and glacial acetic acid (20 mL) added. The reaction was heated to 60 ^{o}C for 5 min before the arylamine (5.50 mmol, 2.3 equiv.) was added and the reaction heated to 120 ^{o}C for 1 h, resulting in a deep red solution. The mixture was then hot-filtered and washed with acetic acid (2 x 10 mL) and Et_2O (2 x 10 mL) to obtain red/yellow zinc chloride complexes of the Ar-BIAN. The zinc chloride complex was then suspended in CH_2Cl_2 (40 mL) and to this mixture was added aqueous sodium oxalate (0.015 M, 20 mL, 2.3 mmol, 1.23 equiv.). The mixture was then shaken for 5 min. The organic layer was then separated and washed with water before drying and removing the solvent under reduced pressure, resulting in red/yellow solid.

N,N'-bis(phenylimino)acenaphthene (Ph-BIAN):

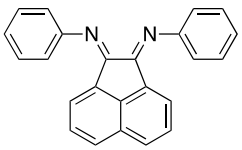

Brown solid (0.19 g). **Yield:** 21%. **Mp:** 191 – 192 ^{o}C. **Litt.:** 191 – 193 ^{o}C.[22a] **^{1}H NMR (300 MHz, $CDCl_3$) δ (ppm):** 7.83 (d, *J* = 8.2 Hz, 1H), 7.41 (t, *J* = 7.7 Hz, 2H), 7.31 (t, *J* = 7.7 Hz, 1H), 7.29 – 7.26 (m, 1H), 7.07 (d, *J* = 0.9 Hz, 2H), 6.77 (d, *J* = 7.2 Hz, 1H). The ^{1}H NMR and Mp matched those found in the literature.[22a]

N,N'-bis(4-fluorophenylimino)acenaphthene (4-FPh-BIAN):

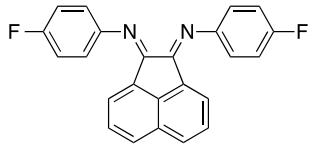

Yellow solid (0.270 g). **Yield:** 27%. **Mp:** 227 – 229 °C. **^{1}H NMR (500 MHz, $CDCl_3$) δ (ppm):** 7.94 (d, *J* = 8.3 Hz, 1H), 7.44 (t, *J* = 7.8 Hz, 1H), 7.20 (t, *J* = 8.5 Hz, 2H), 7.12 (dd, *J* = 8.6, 4.9 Hz, 2H), 6.95 (d, *J* = 7.2 Hz, 1H). **^{19}F NMR (471 MHz, $CDCl_3$) δ (ppm):** -119.24 (s). ^{1}H NMR matched that found in the literature.[37]

N,N'-bis(4-methoxyphenylimino)acenaphthene (4-MeOPh-BIAN):

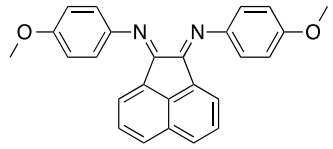

Red solid (0.40 g). **Yield:** 37 %. **Mp:** 189 – 190 °C. Litt.: 189 – 191 °C.[22a] **^{1}H NMR (300 MHz, $CDCl_3$) δ (ppm):** 7.89 (dd, *J* = 8.4, 0.7 Hz, 1H), 7.39 (dd, *J* = 8.3, 7.3 Hz, 1H), 7.14 – 7.06 (m, 2H), 7.05 – 6.99 (m, 2H), 3.89 (s, 3H). The ^{1}H NMR and Mp matched those found in the literature.[22a]

General procedure for the synthesis of [(C^N)Pt(N^N)]PF_6 complexes. Adapted from a protocol by Hasan and Zysman-Colman.[14] $[Pt(C^N)Cl]_2$ (0.13 mmol, 1 equiv.) and Ar-BIAN (0.33 mmol, 2.5 equiv.) were dissolved in CH_2Cl_2 (10 mL). The mixture was degassed and placed under a N_2 atmosphere and heated at reflux for 19 h. The reaction darkened from yellow towards brown over the course of the reaction. The solution was cooled to room temperature and the solvent removed under reduced pressure resulting in a dark brown solid. This crude solid was

redissolved in minimum amount of MeOH and an aqueous solution of NH_4PF_6 (10 mL, 6.13 mL, 1 g/10 mL) was added dropwise with gentle stirring. The resulting brown solid was filtered off and then recrystallised in CH_2Cl_2/Et_2O by vapour diffusion.

[Pt(ppy)(4-MeOPh-BIAN)]PF_6:

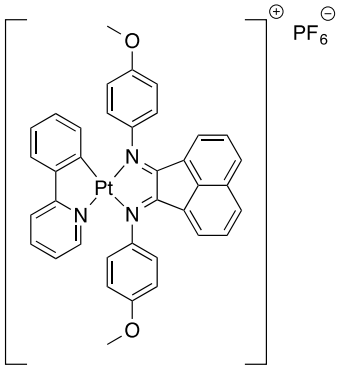

Red-brown solid (0.030 g). **Yield:** 28%. **Mp:** 306 – 307 ^oC. **^{1}H NMR (500 MHz, CD_3CN) δ (ppm):** 8.31 (d, *J* = 8.2 Hz, 2H), 7.90 (td, *J* = 8.0, 1.0 Hz, 1H), 7.82 (d, *J* = 7.9 Hz, 1H), 7.59 (t, *J* = 7.9 Hz, 2H), 7.54 (t, *J* = 8.1 Hz, 1H), 7.48 (s, 4H), 7.29 (d, *J* = 8.3 Hz, 4H), 7.04 (td, *J* = 8.0, 0.5 Hz, 2H), 6.89 (td, *J* = 6.0, 1.5 Hz, 1H), 6.81 (t, *J* = 7.7 Hz, 1H), 5.85 (d, *J* = 8.0 Hz, 1H), 3.98 (s, 6H). **^{19}F NMR (471 MHz, CD_3CN) δ (ppm):** -72.96 (d, *J* = 711 Hz). **LR-MS (ESI) (*m/z*):** 741.1800 (M^+), 681.1595. **HR-MS (ESI):** Calculated ($C_{37}H_{28}N_3O_2Pt$): 741.1829 Found: 741.1800. ***Elemental Analysis (%); Cacld. (found): C 50.12 (49.84); H 3.18 (3.22); N 4.74 (4.60).*** X-ray quality single crystals were obtained through vapour diffusion of CH_2Cl_2/Et_2O.

[Pt(ppy)(Ph-BIAN)]PF_6:

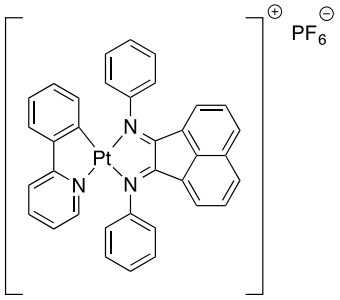

Red-brown solid (0.013 g). **Yield:** 12%. **Mp:** 260 – 265 ^{o}C. **^{1}H NMR (500 MHz, CD_3CN) δ (ppm):** 8.32 (d, *J* = 8.3 Hz, 2H), 7.89 (td, *J* = 7.5, 1.0 Hz, 1H), 7.85 – 7.75 (m, 8H), 7.63 – 7.52 (m, 8H), 7.42 (d, *J* = 6.1 Hz, 1H), 7.03 (t, *J* = 7.5 Hz, 1H), 6.78 (td, *J* = 7.0, 1.0 Hz, 1H), 6.72 (td, *J* = 7.5 1.0 Hz, 1H), 5.71 (d, *J* = 8.1 Hz, 1H). **^{19}F NMR (471 MHz, CD_3CN) δ (ppm):** -72.96 (d, *J* = 711 Hz). **LR-MS (ESI) (*m/z*):** 681.1592 (M^+), 331.1218. **HR-MS (ESI):** Calculated ($C_{35}H_{24}N_3Pt$): 681.1618 Found: 681.1592. ***Elemental Analysis (%); Cacld. (found): C 50.85 (50.67); H 2.93 (2.84); N 5.08 (5.17).***

[Pt(Fppy)(4-MeOPh-BIAN)]PF_6:

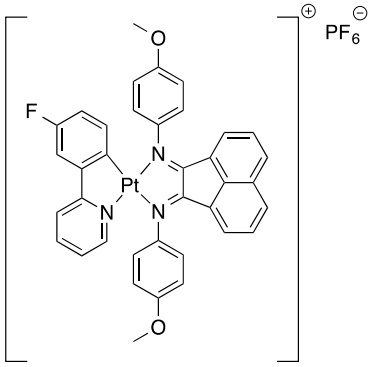

Red-brown solid (0.025 g). **Yield:** 27%. **Mp:** 298 – 300 ^{o}C. **^{1}H NMR (500 MHz, CD_3CN) δ (ppm):** 8.32 (d, *J* = 8.3 Hz, 2H), 7.94 (td, *J* = 7.5, 1.0 Hz, 1H), 7.82 (d, *J* = 8.0 Hz, 1H), 7.60 (t, *J* = 7.9 Hz, 2H), 7.54 (dd, *J* = 6.0, 1.4 Hz, 1H), 7.50 – 7.37 (m, 4H), 7.36 (dd, *J* = 9.8, 2.8 Hz, 1H), 7.29 (d, *J* = 8.5 Hz 4H), 7.08 – 7.02 (m, 1H), 6.93 (ddd, *J* = 7.5, 6.0, 1.5 Hz, 1H), 6.89 – 6.84 (m,

1H), 6.65 (td, *J* = 9.0, 3.0 Hz, 1H), 5.79 (dd, *J* = 8.8, 5.9 Hz, 1H), 3.99 (s, 6H). **^{19}F NMR (471 MHz, CD_3CN) δ (ppm):** -72.96 (d, *J* = 711 Hz), -119.24 (s). **LR-MS (ESI) (m/z):** 759.1707 (M^+), 391.1427. **HR-MS (ESI):** Calculated ($C_{37}H_{27}FN_3O_2Pt$): 759.1730 Found: 759.1707. ***Elemental Analysis (%); Cacld. (found): C 49.12 (48.91); H 3.01 (2.92); N 4.64 (4.78).***

[Pt(3MeOppy)(4-MeOPh-BIAN)]PF_6:

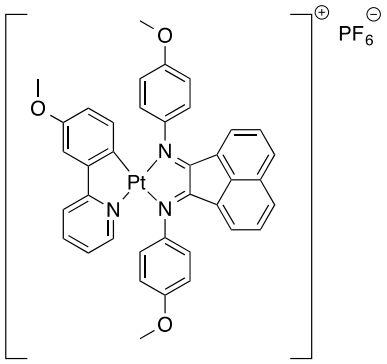

Black-brown solid (0.032 g). **Yield:** 29%. Mp: 254 – 256 °C. **^{1}H NMR (500 MHz, CD_3CN) δ (ppm):** 8.32 (s, 2H), 7.91 (t, *J* = 7.8 Hz, 1H), 7.84 (d, *J* = 8.0 Hz, 1H), 7.65 – 7.40 (m, 7H), 7.29 (d, *J* = 8.3 Hz, 4H), 7.13 (d, *J* = 2.8 Hz, 1H), 7.08 – 7.02 (m, 1H), 6.88 (dd, *J* = 8.8, 7.7 Hz, 2H), 6.48 (dd, *J* = 8.7, 2.8 Hz, 1H), 5.70 (d, *J* = 8.7 Hz, 1H), 3.99 (d, *J* = 4.2 Hz, 6H), 3.75 (s, 3H). **^{19}F NMR (471 MHz, CD_3CN) δ (ppm):** -72.96 (d, *J* = 711 Hz). **LR-MS (ESI) (*m/z*):** 771.1905 (M^+), 741.1809, 393.1583. **HR-MS (ESI):** Calculated ($C_{38}H_{30}N_3O_3Pt$): 771.1935 Found: 771.1905. ***Elemental Analysis (%); Cacld. (found): C 49.79 (49.83); H 3.30 (3.32); N 4.58 (4.68).***

[Pt(ppy)(4-FPh-BIAN)]PF_6:

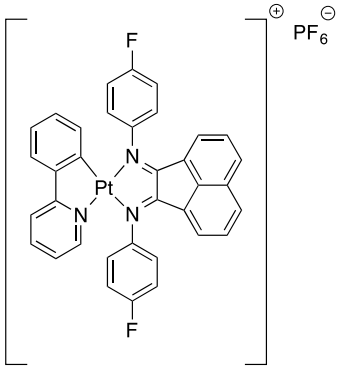

Green-brown solid (0.018 g). **Yield:** 15%. Mp: 296 – 297 ^{o}C. **^{1}H NMR (500 MHz, CD_3CN) δ (ppm):** 8.35 (d, *J* = 8.3 Hz, 2H), 7.92 (td, *J* = 7.8, 1.5 Hz, 1H), 7.84 (d, *J* = 7.5 Hz, 1H), 7.65 – 7.51 (m, 13H), 7.48 (d, *J* = 5.5 Hz, 1H), 7.06 (td, *J* = 7.5, 1.1 Hz, 1H), 6.91 (ddd, *J* = 7.6, 6.1, 1.5 Hz, 1H), 6.83 (td, *J* = 7.7, 1.5 Hz, 1H), 5.77 (d, *J* = 8.0 Hz, 1H). **^{19}F NMR (471 MHz, CD_3CN) δ (ppm):** -72.96 (d, *J* = 711 Hz), -112.39 (d, 2F). **LR-MS (ESI) (*m/z*):** 717.1395 (M^+), 367.1024, **HR-MS (ESI):** Calculated ($C_{35}H_{22}F_2N_3Pt$): 717.1430 Found: 717.1395. ***Elemental Analysis (%); Cacld. (found): C 48.73 (48.79); H 2.57 (2.68); N 4.87 (4.73).*** X-ray quality single crystals were obtained through vapour diffusion of CH_2Cl_2/Et_2O.

Photophysical measurements. All samples were prepared in HPLC grade acetonitrile (MeCN) with varying concentrations on the order of μM. Absorption spectra were recorded at RT using a Shimadzu UV-1800 double beam spectrophotometer. Molar absorptivity determination was verified by linear least-squares fit of values obtained from at least three independent solutions at varying concentrations with absorbance ranging from 15.6 to 338 μM.

Electrochemistry measurements. Cyclic voltammetry (CV) measurements were performed on an Electrochemical Analyzer potentiostat model 600D from CH Instruments. Solutions for cyclic voltammetry were prepared in MeCN and degassed with MeCN-saturated nitrogen bubbling for

about 20 min prior to scanning. Tetra(*n*-butyl)ammoniumhexafluorophosphate ($TBAPF_6$; ca. 0.1 M in MeCN) was used as the supporting electrolyte. A non-aqueous Ag/Ag^+ electrode (silver wire in a solution of 0.1 M KCl in H_2O) was used as the pseudoreference electrode; a Pt electrode was used for the working electrode and a Pt electrode was used as the counter electrode. The redox potentials are reported relative to a normal hydrogen electrode (NHE) electrode with a ferrocenium/ferrocene (Fc^+/Fc) redox couple as an internal reference (Fc/Fc^+ vs NHE = 0.63 V).[24]

X-ray crystallography. Data for complexes **2** and **3** were collected by using a Rigaku FR-X Ultrahigh brilliance Microfocus RA generator/confocal optics and Rigaku XtaLAB P200 system, at 173 K for **2** and 93 K for **3**, using graphite monochromated Mo Kα radiation (λ = 0.71073 Å), and ω steps accumulating area detector images spanning at least a hemisphere of reciprocal space. All data were corrected for Lorentz polarization effects. A multiscan absorption correction was applied by using CrystalClear.[38] Structures were solved by Patterson (PATTY)[39] or direct methods (SIR2004)[40] and refined by full-matrix least-squares against F^2 (SHELXL-2013).[41] Non-hydrogen atoms were refined anisotropically, and hydrogen atoms were refined using a riding model. Compound **2** contained a molecule of CH_2Cl_2 solvent that, on refinement, appeared to be partially occupied. The occupancy of these atoms was fixed at a half. Compound **3** exhibited disorder in the ppy ligand, such that N and C positions were equivalent. This was modelled with equal occupancies for carbon and nitrogen in the same sites. All calculations were performed using the CrystalStructure interface.[42]

References

(1) (a) Baggaley, E.; Weinstein, J. A.; Williams, J. A. G. *Coord. Chem. Rev.* **2012**, *256*, 1762; (b) Liu, Z.; He, W.; Guo, Z. *Chem. Soc. Rev.* **2013**, *42*, 1568.

(2) (a) Costa, R. D.; Ortí, E.; Bolink, H. J.; Monti, F.; Accorsi, G.; Armaroli, N. *Angew. Chem. Int. Ed.* **2012**, *51*, 8178; (b) Ladouceur, S.; Zysman-Colman, E. *Eur. J. Inorg. Chem.* **2013**, *2013*, 2985.
(3) (a) Richter, M. M. *Chem. Rev.* **2004**, *104*, 3003; (b) Hu, L.; Xu, G. *Chem. Soc. Rev.* **2010**, *39*, 3275.
(4) Hagfeldt, A.; Boschloo, G.; Sun, L.; Kloo, L.; Pettersson, H. *Chem. Rev.* **2010**, *110*, 6595.
(5) McDaniel, N. D.; Bernhard, S. *Dalton Trans.* **2010**, *39*, 10021.
(6) Prier, C. K.; Rankic, D. A.; MacMillan, D. W. C. *Chem. Rev.* **2013**, *113*, 5322.
(7) DePriest, J.; Zheng, G. Y.; Goswami, N.; Eichhorn, D. M.; Woods, C.; Rillema, D. P. *Inorg. Chem.* **2000**, *39*, 1955.
(8) Jenkins, D. M.; Senn, J. F., Jr.; Bernhard, S. *Dalton Trans* **2012**, *41*, 8077.
(9) Krikorian, M.; Liu, S.; Swager, T. M. *J Am Chem Soc* **2014**.
(10) (a) Niedermair, F.; Stubenrauch, K.; Pein, A.; Saf, R.; Ingolić, E.; Grogger, W.; Fritz-Popovski, G.; Trimmel, G.; Slugovc, C. *J. Mater. Chem.* **2011**, *21*, 15183; (b) Niedermair, F.; Noormofidi, N.; Lexer, C.; Saf, R.; Slugovc, C. *Polymer* **2011**, *52*, 1874.
(11) Ma, D.-L.; Che, C.-M.; Yan, S.-C. *J. Am. Chem. Soc.* **2008**, *131*, 1835.
(12) Balashev, K. P.; Ivanov, M. A.; Taraskina, T. V.; Cherezova, E. A. *Russ. J. Gen. Chem.* **2006**, *76*, 781.
(13) Kvam, P.-I.; Puzyk, M. V.; Balashev, K. P.; Songstad, J. *Acta Chem. Scand.* **1995**, *49*, 335.
(14) (a) Hasan, K.; Zysman-Colman, E. *Inorg. Chem.* **2012**, *51*, 12560; (b) Hasan, K.; Zysman-Colman, E. *Eur. J. Inorg. Chem.* **2013**, *2013*, 4421.
(15) (a) Shiotsuki, M.; White, P. S.; Brookhart, M.; Templeton, J. L. *J. Am. Chem. Soc.* **2007**, *129*, 4058; (b) Liu, B.; Gao, M.; Dang, L.; Zhao, H.; Marder, T. B.; Lin, Z. *Organometallics* **2012**, *31*, 3410.
(16) Lohr, T. L.; Piers, W. E.; Parvez, M. *Dalton Trans.* **2013**, *42*, 14742.
(17) Parmene, J.; Krivokapic, A.; Tilset, M. *Eur. J. Inorg. Chem.* **2010**, *2010*, 1381.
(18) (a) Adams, C. J.; Fey, N.; Weinstein, J. A. *Inorg. Chem.* **2006**, *45*, 6105; (b) Adams, C. J.; Fey, N.; Harrison, Z. A.; Sazanovich, I. V.; Towrie, M.; Weinstein, J. A. *Inorg. Chem.* **2008**, *47*, 8242; (c) Rachford, A. A.; Hua, F.; Adams, C. J.; Castellano, F. N. *Dalton Trans.* **2009**, 3950.
(19) Crystallographic data for CCDC 1007422-1007423 can be obtained free of charge from The Cambridge Crystallographic Data Centre via http://www.ccdc.cam.ac.uk/data_request/cif.
(20) (a) Blight, B. A.; Ko, S.-B.; Lu, J.-S.; Smith, L. F.; Wang, S. *Dalton Trans.* **2013**, *42*, 10089; (b) Hudson, Z. M.; Sun, C.; Helander, M. G.; Amarne, H.; Lu, Z.-H.; Wang, S. *Adv. Funct. Mater.* **2010**, *20*, 3426; (c) Rao, Y.-L.; Schoenmakers, D.; Chang, Y.-L.; Lu, J.-S.; Lu, Z.-H.; Kang, Y.; Wang, S. *Chem. Eur. J.* **2012**, *18*, 11306; (d) Hudson, Z. M.; Sun, C.; Helander, M. G.; Chang, Y.-L.; Lu, Z.-H.; Wang, S. *J. Am. Chem. Soc.* **2012**, *134*, 13930.
(21) Baker, G. A.; Rachford, A. A.; Castellano, F. N.; Baker, S. N. *Chemphyschem* **2013**, *14*, 1025.
(22) (a) Hasan, K.; Zysman-Colman, E. *J. Phys. Org. Chem.* **2013**, *26*, 274; (b) Gasperini, M.; Ragaini, F.; Cenini, S. *Organometallics* **2002**, *21*, 2950.
(23) Li, L.; Brennessel, W. W.; Jones, W. D. *Organometallics* **2009**, *28*, 3492.
(24) Pavlishchuk, V. V.; Addison, A. W. *Inorg. Chim. Acta* **2000**, *298*, 97.
(25) (a) Janzen, D. E.; VanDerveer, D. G.; Mehne, L. F.; da Silva Filho, D. A.; Bredas, J.-L.; Grant, G. J. *Dalton Trans.* **2008**, 1872; (b) Ghedini, M.; Pugliese, T.; La Deda, M.; Godbert, N.; Aiello, I.; Amati, M.; Belviso, S.; Lelj, F.; Accorsi, G.; Barigelletti, F. *Dalton Trans.* **2008**, 4303.

(26) (a) Wong, W.-Y.; Wang, X.-Z.; He, Z.; Chan, K.-K.; Djurišić, A. B.; Cheung, K.-Y.; Yip, C.-T.; Ng, A. M.-C.; Xi, Y. Y.; Mak, C. S. K.; Chan, W.-K. *J. Am. Chem. Soc.* **2007**, *129*, 14372; (b) Wu, W.; Zhang, J.; Yang, H.; Jin, B.; Hu, Y.; Hua, J.; Jing, C.; Long, Y.; Tian, H. *J. Mater. Chem.* **2012**, *22*, 5382; (c) Islam, A.; Sugihara, H.; Hara, K.; Singh, L. P.; Katoh, R.; Yanagida, M.; Takahashi, Y.; Murata, S.; Arakawa, H.; Fujihashi, G. *Inorg. Chem.* **2001**, *40*, 5371; (d) Geary, E. A. M.; McCall, K. L.; Turner, A.; Murray, P. R.; McInnes, E. J. L.; Jack, L. A.; Yellowlees, L. J.; Robertson, N. *Dalton Trans.* **2008**, 3701.
(27) (a) Brooks, J.; Babayan, Y.; Lamansky, S.; Djurovich, P. I.; Tsyba, I.; Bau, R.; Thompson, M. E. *Inorg. Chem.* **2002**, *41*, 3055; (b) Kvam, P.; Puzyk, M. V.; Balashev, K. P.; Songstad, J.; Lundberg, C.; Arnarp, J.; Björk, L.; Gawinecki, R. *Acta Chem. Scand.,* **1995**, *49*, 335.
(28) (a) Rosa, V.; Avilés, T.; Aullon, G.; Covelo, B.; Lodeiro, C. *Inorg. Chem.* **2008**, *47*, 7734; (b) Rosa, V.; Santos, C. I. M.; Welter, R.; Aullón, G.; Lodeiro, C.; Avilés, T. *Inorg. Chem.* **2010**, *49*, 8699; (c) Paulovicova, A.; El-Ayaan, U.; Shibayama, K.; Morita, T.; Fukuda, Y. *Eur. J. Inorg. Chem.* **2001**, *2001*, 2641.
(29) Dai, F.-R.; Chen, Y.-C.; Lai, L.-F.; Wu, W.-J.; Cui, C.-H.; Tan, G.-P.; Wang, X.-Z.; Lin, J.-T. s.; Tian, H.; Wong, W.-Y. *Chem. Asian J.* **2012**, *7*, 1426.
(30) Graham, K. R.; Yang, Y.; Sommer, J. R.; Shelton, A. H.; Schanze, K. S.; Xue, J.; Reynolds, J. R. *Chem. Mater.* **2011**, *23*, 5305.
(31) Rausch, A. F.; Murphy, L.; Williams, J. A. G.; Yersin, H. *Inorg. Chem.* **2011**, *51*, 312.
(32) Li, W.; Nelson, D. P.; Jensen, M. S.; Hoerrner, R. S.; Cai, D.; Larsen, R. D.; Reider, P. J. *J. Org. Chem.* **2002**, *67*, 5394.
(33) Kuivila, H. G.; Wiles, R. A. *J. Am. Chem. Soc.* **1955**, *77*, 4830.
(34) Kajimoto, O.; Saeki, T.; Nagaoka, Y.; Fueno, T. *J. Phys. Chem.* **1977**, *81*, 1712.
(35) Vandromme, L.; Reißig, H.-U.; Gröper, S.; Rabe, J. P. *Eur. J. Org. Chem.* **2008**, *2008*, 2049.
(36) Campeau, L.-C.; Rousseaux, S.; Fagnou, K. *J. Am. Chem. Soc.* **2005**, *127*, 18020.
(37) Sprengers, Jeroen W.; de Greef, M.; Duin, Marcel A.; Elsevier, Cornelis J. *Eur. J. Inorg. Chem.* **2003**, *2003*, 3811.
(38) *CrystalClear-SM Expert v. 2.1*; The Woodlands, Texas, USA, **2010-2013**
(39) Beurskens, P. T.; Beurskens, G.; de Gelder, R.; Garcia-Granda, S.; Gould, R. O.; Israel, R.; Smits, J. M. M. *DIRDIF-99*; University of Nijmegen, The Netherlands, **1999**
(40) Burla, M. C.; Caliandro, R.; Camalli, M.; Carrozzini, B.; Cascarano, G. L.; De Caro, L.; Giacovazzo, C.; Polidori, G.; Spagna, R. *J. Appl. Crystallogr.* **2005**, *38*, 381.
(41) Sheldrick, G. *Acta Crystallographica Section A* **2008**, *64*, 112.
(42) *CrystalStructure v4.1.* ; The Woodlands, Texas, USA, , **2013**

TOC graphic.

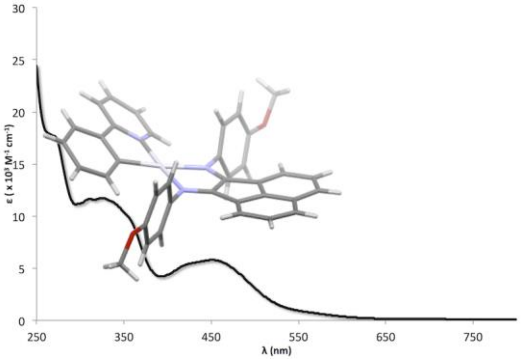
30
25
20
15
10
5
0
ε (x 10³ M⁻¹ cm⁻¹)
250
350
450
550
650
750
λ (nm)